Arabian Journal of Chemistry (2020) 13, 3344–3350

King Saud University

Arabian Journal of Chemistry

www.ksu.edu.sa
www.sciencedirect.com

ORIGINAL ARTICLE

# Bandgap engineering of $TiO_2$ nanoparticles through MeV Cu ions irradiation

**Ishaq Ahmad [a,b,h,i,*], Muhammad Usman [a], Ting-kai Zhao [b,c], Sara Qayum [a,d], Iram Mahmood [f], Arshad Mahmood [e], Abdoulaye Diallo [g,h,i], Camillus Obayi [j], Fabian Ifeanyichukwu Ezema [h,i,k,*], Malik Maaza [h,i]**

[a] *Experimental Physics Labs, National Centre for Physics, Quaid-i-Azam University Campus, Islamabad 44000, Pakistan*
[b] *NPU-NCP Joint International Research Center on Advanced Nanomaterials and Defects Engineering, Northwestern Polytechnical University, Xi'an 710072, China*
[c] *School of Materials Science & Engineering, Northwestern Polytechnical University, Xi'an 710072, China*
[d] *Physics Department, Allama Iqbal Open University, Islamabad, Pakistan*
[e] *National Institute of Lasers and Optronics (NILOP), P.O Nilore, Islamabad, Pakistan*
[f] *Department of Industrial Engineering, College of Engineering, King Khalid University, Abha 61413, Saudi Arabia*
[g] *Department of Physics and Chemistry, Faculty of Sciences and Technologies of Formation and Education, University Cheikh Anta Diop (UCAD), B.P. 5036 Dakar-Fann, Senegal*
[h] *UNESCO-UNISA Africa Chair in Nanosciences/Nanotechnology, College of Graduate Studies, University of South Africa, Muckleneuk Ridge, PO Box 392, Pretoria, South Africa*
[i] *Nanosciences African Network (NANOAFNET), iThemba LABS, National Research Foundation, P O Box 722, Somerset West 7129, South Africa*
[j] *Department of Metallurgical & Materials Engineering, University of Nigeria, Nsukka 410001, Enugu State, Nigeria*
[k] *Department of Physics & Astronomy, University of Nigeria, Nsukka 410001, Enugu State, Nigeria*

Received 6 September 2018; accepted 8 November 2018
Available online 14 November 2018

**KEYWORDS**

$TiO_2$ nanoparticles;
$Cu^{++}$ irradiation;
Rutile phase;
Coalescence of NPs;
Bandgap engineering

**Abstract** The effect of 5 MeV $Cu^{++}$ ions irradiation on structural and optical properties of Anatase $TiO_2$ nanoparticles ($TiO_2$-NPs) is investigated. For this purpose, $TiO_2$-NPs are irradiated with different $Cu^{++}$ ions fluences, ranging from $1 \times 10^{15}$ to $1 \times 10^{16}$ ions/cm$^2$ at room temperature. XRD results confirm the $Ti_3O_7$ phase appear at the dose of $5 \times 10^{15}$ ions/cm$^2$ and peak intensity of $Ti_3O_7$ phase gradually increases with an increase of $Cu^{++}$ ions irradiation dose. At the dose of $1 \times 10^{16}$ ions/cm$^2$ $TiO_2$ Anatase phase were transformed to Rutile phase. Same observations are confirmed from Raman spectroscopy. High resolution transmission electron microscopy

* Corresponding authors at: UNESCO-UNISA Africa Chair in Nanosciences/Nanotechnology, College of Graduate Studies, University of South Africa, Muckleneuk Ridge, P O Box 392, Pretoria, South Africa.
E-mail addresses: ishaq@ncp.edu.pk (I. Ahmad), fabian.ezema@unn.edu.ng (F.I. Ezema).
Peer review under responsibility of King Saud University.

Production and hosting by Elsevier

https://doi.org/10.1016/j.arabjc.2018.11.008

(HRTEM) reveals that morphology converted into wavy shape and crystal structure detrioted with increase Cu ion irradiation dose to form vacancy loops and interstitial loops. Scanning electron microscopy (SEM) shows that $TiO_2$-NPs have been fused to form a cluster of nanoparticles at high Cu ion beam dose, while bandgap of $TiO_2$-NPs reduces from 3.19 eV to 2.96 eV as a function of $Cu^{++}$ irradiation fluence. These phase transformations and crystal damage are the responsible for optical bandgap reduction. The mechanism for the currently observed phase transformation of $TiO_2$ and coalescence of $TiO_2$-NPs are discussed in term of thermal spikes model.



## 1. Introduction

Titanium dioxide ($TiO_2$), commonly known as titania, had been the focus of research from past several years for various applications such as optical coatings, solar energy conversions, gas sensing materials, catalysis, energy storage, and medicines. Apart from its multidimensional application, nano-crystalline titania $TiO_2$ is a promising candidate for the chemical and mechanical industries(Fujishima and Honda, 1972). The material properties of $TiO_2$-NPsare dependent on the crystal structure, nanoparticle size, and morphology. An interesting feature of $TiO_2$ is its availability in three different crystal phases; brookite, anatase, and rutile. Anatase and rutile are commonly available polymorphs of $TiO_2$, whereas brookite is observed as a by-product along with anatase and rutile or both phases (Li and Ishigaki, 2004). In rutile phase the opposing edges of tetrahedron are in shearedforms that create a linear chain along [0 0 1]. While in anatase phase there is no sharing rather having 4 edges that are shared per octahedral Wall, 1984. The phase changing aspects of $TiO_2$ are strongly related to the crystal structures. Therefore, any alternation in the structure or morphology of $TiO_2$-NPsthrough external means may result in different characteristics of the material, which can be exploited for various applications (see Table 1).

$TiO_2$ falls in the category of wide bandgap materials and has enormous potential to be exploited in developing wide range of applications. However, due to large band gap (3.0 eV to 3.4 eV) only UV light can be harvested which is less than 5% in natural sunlight. Since, photo induced electrons and holes can easily get coupled, subsequently insignificant availability for activity results in the reduction of performance of device. It is of great desire to utilize both UV irradiation (290–400 nm) and visible light (400–700 nm) to improve the device efficiency, which is possible by band gap engineering. Therefore, by reducing the bandgap of $TiO_2$ nanoparticles, the performance of energy storage and conversion devices can be enhanced Xie et al., 2018; Dette et al., 2014; Khan and Khan, 2018.

Ion irradiation is one of technique which is utilized to change the morphology of the material through the interaction of energetic ions with the target material (Ishaq et al., 2013; Khan et al., 2016). It has been proved to be a method of tailoring the bandgap in various materials, by defect-induced impurity states Ahmad et al., 2014; Usman et al., 2015; Usman et al., 2017; Li et al., 2012. The defects produced through ion irradiation conduct through hoping mechanism, which also reduce the resistivity of the material Usman et al., (2009). In $TiO_2$, tailoring of the bandgap has applications in various application areas, such as solar cells Luo et al., 2014; Hsu et al., 2015, where reduced bandgap enables the materials to absorb visible region of light instead of only UV region, which is only permitted by the intrinsic bandgap. The tailoring of the $TiO_2$ bandgap through ion irradiation has previously been explored to some extent using various ion species which has been summarized in ref. Stepanov, (2012). Additionally, ion implanted or irradiation induced defects in $TiO_2$ have extensively been investigated through hydrogen (Heidari et al., 2015), Fe (Leedahl et al., 2014; Impellizzeri et al., 2014), Hg (Khubeis et al., 1998), Xe (Hartmann et al., 1998), O (Rukade et al., 2013), Ge and Si (Zhou et al., 2011) irradiations.

In the present work the $TiO_2$-NPswere irradiated by5 MeV Cu ionsfor different fluences. The effect of Cu irradiation was investigated through transmission electron microscopy (TEM), x-ray diffraction (XRD) structurally whereas diffuse reflectance spectroscopy (DRS) and Raman spectroscopy were implied to see optical response. The band gap variations were studied by interpreting the DRS data and it was observed that the bandgap of $TiO_2$ is reduced from 3.26 eV to 2.96 eV because of irradiation induced structural modifications in the nanoparticles.

**Table 1** Crystalline size against various fluences of Cu ions.

| Sample | Crystallite size (nm) |
|---|---|
| $1 \times 10^{15}$ ions/cm$^2$ | 10.2622 |
| $5 \times 10^{15}$ ions/cm$^2$ | 20.5162 |
| $1 \times 10^{16}$ ions/cm$^2$ | 21.6627 |

## 2. Experimental procedure

The $TiO_2$-NPsused in the present investigation were purchased from Sigma Aldrich and had a diameter of 120 nm. $TiO_2$-NPswere dispersed in isopropanol and then spray coated on glass substrates placed on a hot plate at 170 °C for rapid evaporation of isopropanol. $TiO_2$-NPsfilm were formed on glass substrate by and later cut into $1 \times 1$ cm$^2$ pieces to ensure that all samples have the same physical properties. The prepared $TiO_2$ nanoparticles' thin films were irradiated with 5 MeV Cu ions with different fluences ranging from $1 \times 10^{15}$ to $1 \times 10^{16}$ ions/cm$^2$ at room temperature. The ion irradiation was performed using Pelletron Tandem accelerator at National Centre for Physics, Islamabad, Pakistan. High energy heavy Cu ions were selected in such a way that maximum defects are produced in nanostructures by the ions while traversing through the films, and imparting energy to the nanoparticles

in the form of ionization and collision cascade. During irradiation, the vacuum of the target chamber was kept at $\sim 10^{-7}$ Pa and a controlled current of ions was supplied.

The morphology of un-irradiated and irradiated $TiO_2$-NPsthin film was observed by TEM whereas, structural properties were studied before and after irradiation of $TiO_2$ nanoparticles thin film using HRTEM, XRD and Raman spectroscopy. The optical properties were measured by a diffused reflectance spectroscopy (DRS) and the band gap was calculated afterwards.

## 3. Results and discussion

### 3.1. TEM, HRTEM, EDX and SAED study

Fig. 1(a) shows TEM image of un-irradiated $TiO_2$-NPsdispersed on copper grid whereas Fig. 1b is the corresponding EDX, which confirms the material constituents of the nanoparticle film. It is seen that Ti is present at two different x-ray energies. The Ti peak at 4.5 keV correspond to Ti ($K_\alpha$) and a relatively shorter peak at about 4.9 keV ($K_\beta$). In addition, Cu is also seen in the spectrum, which probably is coming from the Cu grid. The presence of stronger peak of oxygen at lower energies is from $TiO_2$ with some carbon associated with it, which is expected to be from surface.

Fig. 1c is HRTEM image showing that the nanoparticles are not in highly quality crystalline form. Crystal planes are visible as shown in inset of Fig. 1c. Fig. 1d is corresponding SAED image of various hkl values of the $TiO_2$. It can be seen that there are few bright spots representing crystallinity with scattered dull spots which refer polycrystallinity of the nanoparticles. It can be concurred from these results that the as-received form of $TiO_2$-NPs is of mixed phase of crystalline as well as polycrystalline with high purity.

Fig. 2 shows the effect of 5 MeV $Cu^{++}$ irradiation on $TiO_2$-NPswith lower ion fluence of $1 \times 10^{15}$ ions/cm$^2$. The morphology as well as structure was observed as could be observed in Fig. 2a, and b. Morphology starts becoming undulated. Points defects are created while crystal planes are existing with slightly damaged structure. Similar structural damage of ZnO nanowires by proton beam irradiation was observed by C. F. Dee et al (Dee et al., 2011). Ishaq et al also observed that ion beam created defects in multi-walled carbon nanotubes and explained that damage structure due to ion beam induced collision cascade effect Ahmad and Yan, 2009; Ahmad et al., 2009.

Further increase in $Cu^{++}$ irradiation fluence to $5 \times 10^{15}$ -ions/cm$^2$, the morphology, i.e. size of nanoparticles remained unchanged (as seen in Fig. 3a) but surface is undulated and crystalline planes are disturbed as shown in Fig. 3b. Undulated surface morphology was observed previously on ZnO nano-

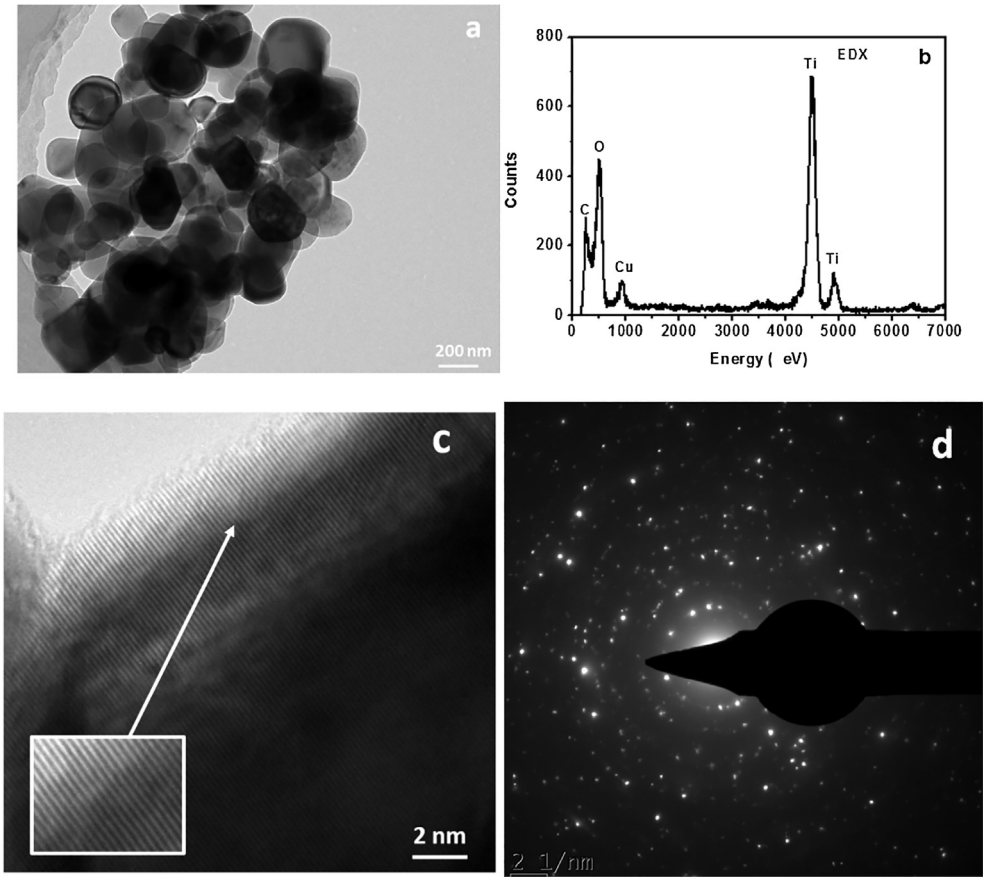


**Fig. 1** Un-irradiation $TiO_2$ (a) TEM: Morphology of $TiO_2$-NPs, (b) EDX spectrum indicating absence of any impurity, (c) HRTEM image showing crystal as well as polycrystalline phases, (d) SAED image representing bright and blurry spots indicating mixed crystalline and polycrystalline phases.

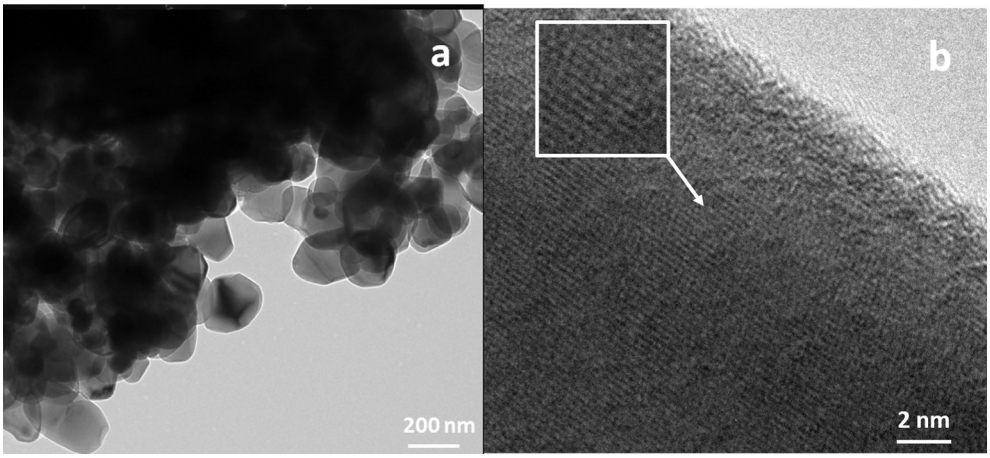


**Fig. 2** $1 \times 10^{15}$ ions/cm$^2$ irradiation $TiO_2$ (a) TEM: Morphology of $TiO_2$-NPs, (b) HRTEM image showing crystalline quality.

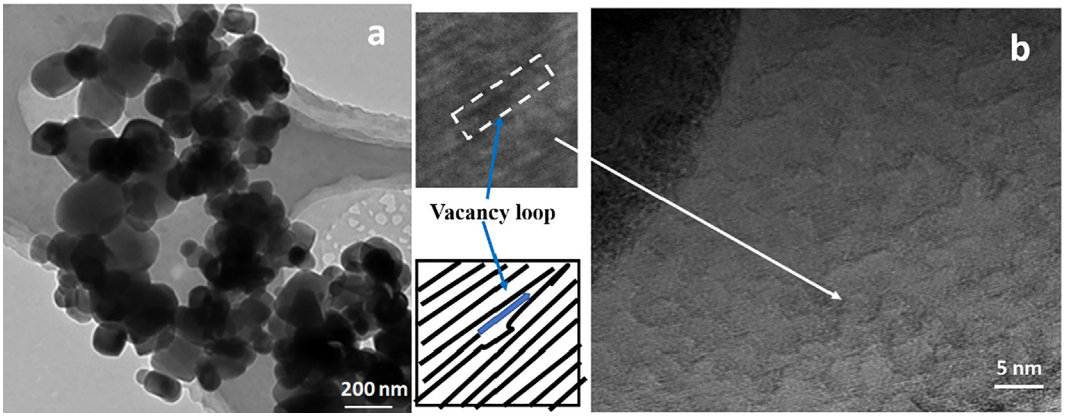


**Fig. 3** $5 \times 10^{15}$ ions/cm$^2$ irradiation $TiO_2$ (a) TEM: Morphology of $TiO_2$-NPs, (b) HRTEM image showing crystalline quality.

wires by ion beam irradiation(Ishaq et al., 2013). Fig. 3b clearly shows that point defects such as vacancies created by Cu ions and these vacancies agglomerated to form vacancy loops due to increase ion dose.

Increasing the $Cu^{++}$ fluence to $1 \times 10^{16}$ ions/cm$^2$ leaves different results. Fig. 4a shows the TEM image of $TiO_2$-NPs. Here it can be observed that few nanoparticles have been fused to form a cluster of nanoparticles. This fusion of particles is the consequence of thermal spike generated by high energy Cu atoms traversing through the nanoparticle. Coalescence of nanowires and nanotubes were observed previously by ion beam irradiation Honey et al., 2017; Honey et al., 2017; Shehla et al., 2016; Shehla et al., 2016; Honey et al., 2015; Ahmad et al., 2011. On the other hand, the crystallinity of the material is detrioted and interstitial defects are observed which ultimately agglomerate to forms interstitials loops as shown in Fig. 4b.

### *3.2. XRD analysis*

Fig. 5 shows the XRD results of un-irradiated, and $Cu^{++}$ irradiated TiO2-NPs. It is observed that different fluences of Cu ions induce reduction of $TiO_2$. The spectrum in black shows the XRD results of reference samples (Fig. 5a), which were irradiated later. The spectrum in red shows the $TiO_2$ at the ion $1 \times 10^{15}$ ions/cm$^2$, blue is of the applied fluence of $5 \times 10^{15}$ ions/cm$^2$ and the spectrum in purple is radiated with applied dose $1 \times 10^{16}$ ions/cm$^2$. The spectrum analysis gives a hint of the partial phase transition from $TiO_2$ anatase to $TiO_2$ Rutile structure, due to the appearance of new planes in the spectrum, however, it is not clear if these planes appear due to the defects in the material or due to phase change. Fig. 5b shows a small shift in the xrd peak around 37.3 to 38.2 degrees, which reflects the change in lattice constant, mainly due to defects in the material. In addition, $Ti_3O_7$ is observed in xrd analysis of irradiated samples.

For the structural matching the XRD patterns of the samples in Fig. 5b are labelled as dose 1, dose 2 and dose 3 for different ion fluences in increasing order. The patterns were matched with the standard data JCPDS file No.894921 for all three samples having tetragonal unit cell with space group $14_1$/amd (1 4 1) and formula unit 4 which confirmed the formation of single phase $TiO_2$-NPsin the samples. However, some extra peaks are observed which point out the presence of TiO and $Ti_3O_5$ phases according to the JCDPS files numbers 85-2084 and 89-4733 respectively. Ishaq et al. observed such kind of phase transformation of boron nitride nanotubes and InGaN thin films by ion beam irradiation Ahmad et al.,

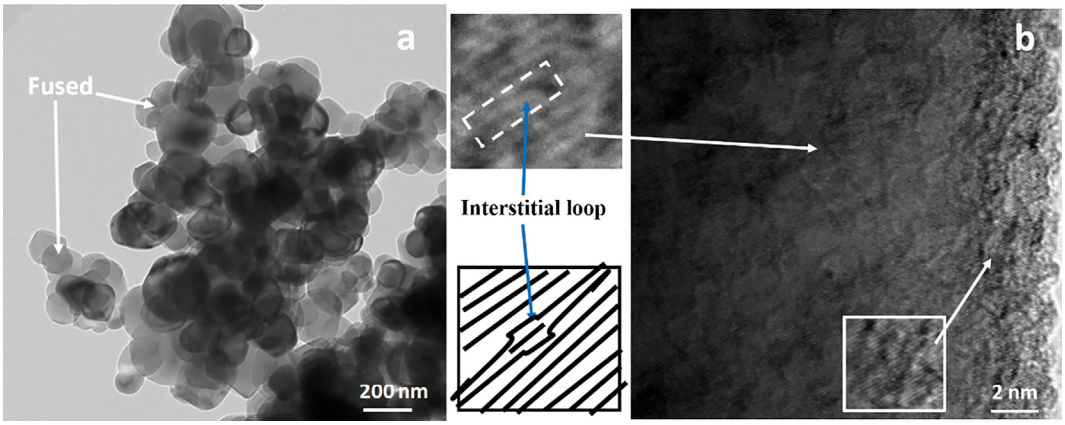


**Fig. 4** $1 \times 10^{16}$ ions/cm$^2$ irradiation $TiO_2$ (a) TEM: Morphology of $TiO_2$-NPs, (b) HRTEM image showing crystalline quality,

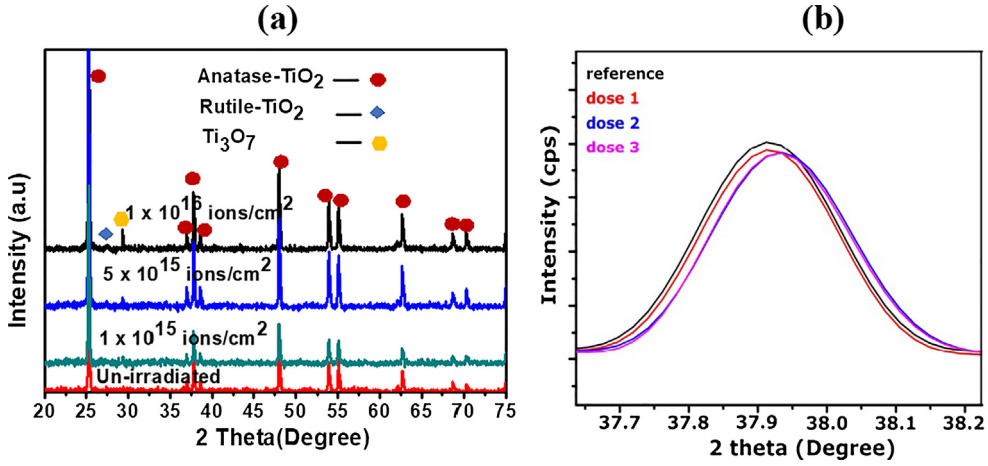


**Fig. 5** (a) XRD pattern of un-irradiated, $1 \times 10^{15}$ (dose 1), $5 \times 10^{15}$(dose 2) and $1 \times 10^{16}$ cm$^{-2}$ (dose 3) irradiated $TiO_2$-NPs, (b) Main peak of Anatase phase of $TiO_2$.

2014; Ahmad et al., 2017 The mean crystallite sizes were estimated for all the samples using high intensity peak (1 0 1) with the help of Debye-Scherrer formula:

$$D = K\lambda/\beta\cos\theta$$

where D is the average crystallite size, 'K' is the Scherrer constant (0.89), λ is the wavelength of the X-ray radiation used (1.54 nm), β is the angular line width at half- maximum intensity and θ is Bragg's angle of the (1 0 1) main peak in degree unit. The results of corresponding sizes are enlisted in the table.

From the table it is shown that by increasing $Cu^{++}$ fluence the mean size of $TiO_2$-NPsalso increases that can be attributed to the fluences assisted crystal growth and/or the redistribution of cations among the interstitial sites.

### 3.3. Optical measurements

Fig. 6 shows the DRS spectrum of un-irradiation and $Cu^{++}$-irradiated $TiO_2$-NPsfilms. The reflectance for the reference is close to 100 percent at 415 nm. After the irradiation fluences a sharp decrease in the reflectance up to 55% at 380 nm for$1 \times 10^{15}$ ions/cm$^2$ and for $5 \times 10^{15}$ ions/cm$^2$ the reflectance is at 58% at 390 nm. While for $1 \times 10^{16}$ ions/cm$^2$ the reflectance sharply decreases to 24% at approximately 390 nm. This shows that the ion fluence has increased the transmission of light through the nanoparticles films leading it to be able to absorb light. Additionally, a clear variation of reflectance under different ion fluences reflects the engineering of the band structure of $TiO_2$, which predicts the phase shifts in the $TiO_2$ under different irradiation circumstances.

From reflectance measurements, it is possible to calculate bandgap thorough K-M Function. In order to determine the bandgap, the spectra was fitted with K-M function.

$$F(R) = (1 - R)^2/2R$$

where R is absolute value of reflectance. The fitted values of bandgap are plotted in Fig. 6c. The bandgap is calculated through curve fitting of reflectance data, and it is compared with $TiO_2$ reference along with the irradiated samples. For the reference the band energy is calculated 3.21 eV, for $1 \times 10^{15}$ ions/cm$^2$ is 3.19 eV, for $5 \times 10^{15}$ ions/cm$^2$ the band energy is 3.16 eV, while for the $1 \times 10^{16}$ ions/cm$^2$ the band gap energy is observed to be 2.96 eV. Theseresults show that by applying differentfluences of Cu ions onto the $TiO_2$-NPs, the band gap can be altered, which is dependent on the fluence of ions. The effect is even stronger for highest fluence of ions. With this trend of tailoring of $TiO_2$ bandgap by ion beam irra-

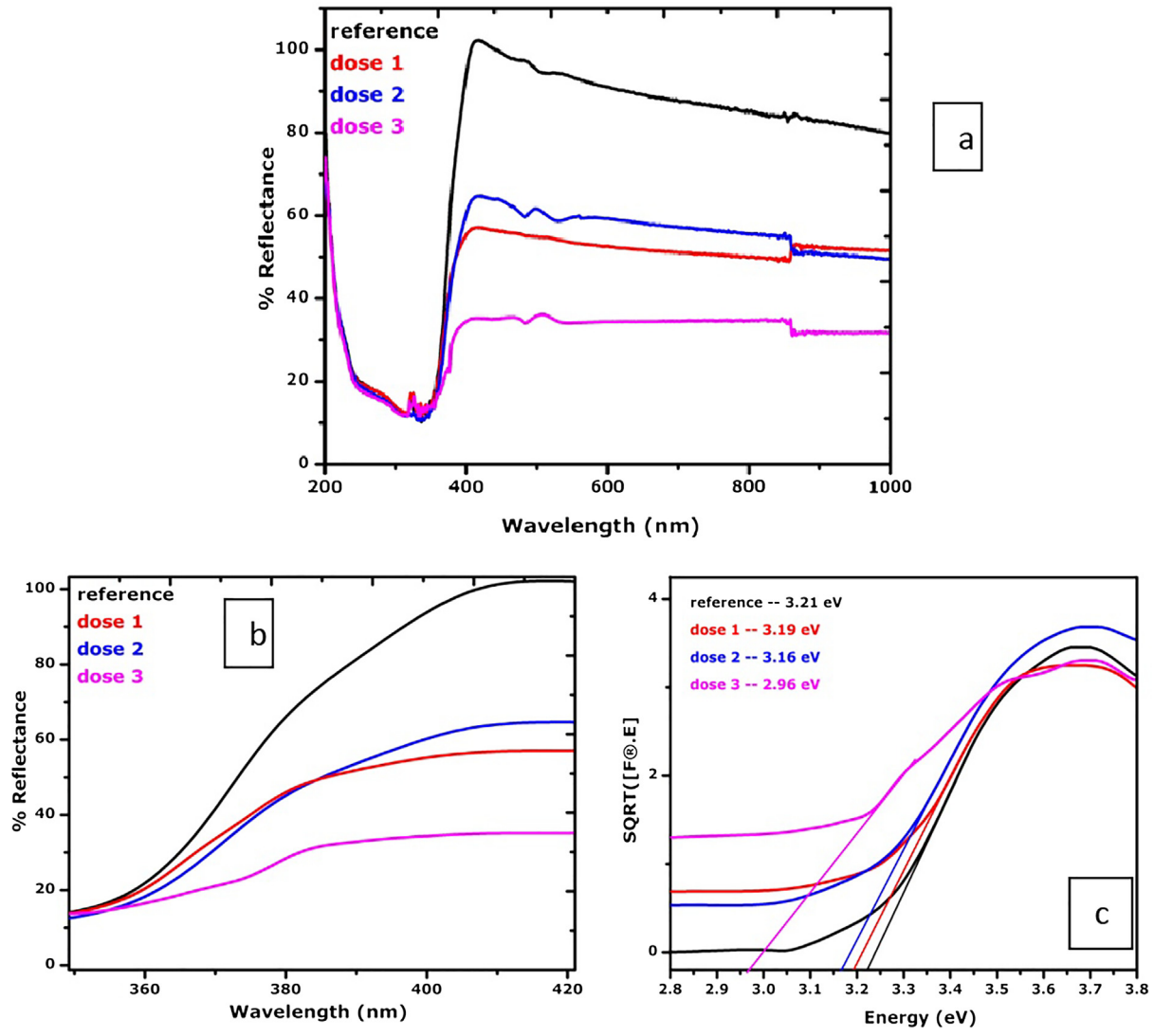


**Fig. 6** (a and b) DRS spectrum of $TiO_2$ under Cu irradiationfluences and (c) corresponding band gap energy.

diation, the nanoparticle material can be enabled to absorb visible wavelengths of the electromagnetic spectrum, resulting in the enhancement of the optical properties of TiO2 (Bin Mo et al., 105, (2014).). These tailored nanoparticles can be used in energy storage, energy harvesting and photocatalytic applications (Xie et al., 2018; Dette et al., 2014; Khan and Khan, 2018).

### *3.4. Raman spectroscopy*

The Raman spectra for the $TiO_2$ un-irradiated and irradiated samples are shown in the Fig. 7. The spectra show different crystalline phases of $TiO_2$. The anatase and rutile crystallize respectively in tetragonal space group where their unit cells have 4 and 2 $TiO_2$ formula structures. In Fig. 7 the main peak of $E_g$ mode for anatase is at 148 $cm^{-1}$, while in B1g mode of rutile after the irradiation it shifts towards 157.7 $cm^{-1}$. Also for anatase to rutile the clear shift can be seen in the figure at 519 $cm^{-1}$ in the reference and 505 $cm^{-1}$, 503 $cm^{-1}$, and 499 $cm^{-1}$. This could be the reason that the Raman spectra

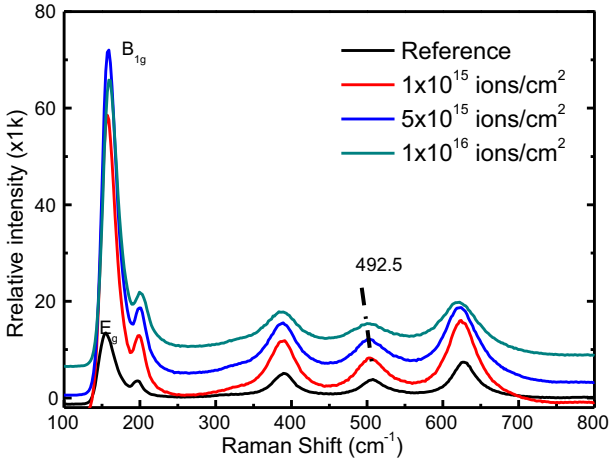


**Fig. 7** Raman Spectra of $TiO_2$.

of anatase phase of irradiated samples quickly changes and sharp peaks can be seen for $Cu^{++}$ fluence1 $\times 10^{15}$, $5 \times 10^{15}$ and $1 \times 10^{16}$ $cm^{-2}$. The $E_g$ mode is in anatase phase while $B1_g$ modes show the rutile phase of $TiO_2$.

## 4. Summary

$TiO_2$ nanoparticles were deposited on glass substrate in the form of thin film. These films were bombarded by 5 MeV Cu ions with various fluences at room temperature. The energetic Cu ions transferred their energy to $TiO_2$-NPsand made changes in the structure and optical response of the material. It is seen that the structure of the nanoparticles changes from crystalline to amorphous at few places, as observed through HR-TEM. However, the crystal planes were still observable in XRD even for higher fluences of Cu ions. It is observed that un-irradiated XRD spectrum shows anatase nature of $TiO_2$-NPs, while after irradiation at the fluence of $1 \times 10^{15}$ ions/$cm^2$, anatase structure was transform to rutile and $Ti_3O_7$ phases. As a consequence of Cu irradiation, it is clearly seen that the bandgap of $TiO_2$-NPschange from 3.19 eV to 2.96 eV, which has application in various fields.

## Acknowledgments

iThemba LABS, UNESCO and TWAS are gratefully acknowledged. We are grateful to deanship of scientific research at King Khalid University, Abha Kingdom of Saudi Arabia for technical and administrative support. FIE graciously knowledge UNISA for VRSP Fellowship (90407830) award. Fabian Ezema acknowledges the award of grant by TETFUND under contract number TETF/DESS/UNN/NSUKKA/STI/VOL.I/B4.33.

Plagiarism has been carried out via ID 940538612 (similarity index 9%) in Turnitin software.

## References:

Fujishima, A., Honda, K., 1972. Nature 238, 37.
Li, J.-G., Ishigaki, T., 2004. Acta Mater. 52, 5143.
Wall, A.F., 1984. Structural Inorganic Chemistry. Oxford University Press.
Ishaq, A., Usman, M., Dee, C.F., Khurram, A.A., Yan, L., Zhou, X. T., Nadeem, A., Naseem, S., Rafique, H.M., Majlis, B.Y., 2013. J. Nanoparticle Res. 15, 1.
Khan, S.A., Ziya, A.B., Ibrahim, A., Atiq, S., Usman, M., Ahmad, N., Shakeel, M., 2016. J. Electron. Mater. 45, 2258.
Ahmad, I., Usman, M., Rabab Naqvi, S., Iqbal, J., Bo, L., Long, Y., Dee, C.F., Baig, A., 2014. J. Nanoparticle Res. 16.
Usman, M., Naeem, M., Hassan, N.U., Maqbool, M., Ahmad, I., Ahmad, I., Hussain, Z., 2015. Appl. Surf. Sci. 357, 179.
Usman, M., Khan, S., Khan, M., Abbas, T.A., 2017. Appl. Surf. Sci. 392, 863.
Li, X., Wu, X., Zeng, X.C., Yang, J., 2012. ACS Nano 6, 4104.
Usman, M., Nazir, A., Aggerstam, T., Linnarsson, M.K., Hallén, A., 2009. Nucl. Instrum. Methods Phys. Res. Sect. B Beam Interact. Mater. Atoms 267, 1561.
Luo, J., Zhou, J., Guo, H., Yang, W., Liao, B., Shi, W., Chen, Y., 2014. RSC Adv. 4, 56318.
Hsu, W., Sutter-Fella, C.M., Hettick, M., Cheng, L., Chan, S., Chen, Y., Zeng, Y., Zheng, M., Wang, H.-P., Chiang, C.-C., Javey, A., 2015. Sci. Rep. 5, 16028.
Stepanov, A.L., 2012. Rev. Adv. Mater. Sci. 30, 150.
Heidari, S., Mohammadizadeh, M.R., Mahjour-Shafiei, M., Larijani, M.M., Malek, M., 2015. Appl. Phys. A 121, 149.
Leedahl, B., Zatsepin, D.A., Boukhvalov, D.W., Green, R.J., McLeod, J.A., Kim, S.S., Kurmaev, E.Z., Zhidkov, I.S., Gavrilov, N.V., Cholakh, S.O., Moewes, A., 2014. J. Appl. Phys. 115.
Impellizzeri, G., Scuderi, V., Romano, L., Sberna, P.M., Arcadipane, E., Sanz, R., Scuderi, M., Nicotra, G., Bayle, M., Carles, R., Simone, F., Privitera, V., 2014. J. Appl. Phys. 116.
Khubeis, I., Fromknecht, R., Massing, S., Meyer, O., 1998. Nucl. Instrum. Methods Phys. Res. Sect. B Beam Interact. Mater. Atoms 141, 332.
Hartmann, T., Wang, L.M., Weber, W.J., Yu, N., Sickafus, K.E., Mitchell, J.N., 1998. Nucl. Instrum. Methods Phys. Res. Sect. B Beam Interact. Mater. Atoms 141, 398.
Rukade, D.A., Desai, C.A., Kulkarni, N., Tribedi, L.C., Bhattacharyya, V., 2013. AIP Conf. Proc. 1512, 380.
Zhou, Y., He, F., Huang, Y., Wan, Y., Wang, Y., 2011. Int. J. Mod. Phys. B 25, 1629.
Bin Mo, L., Bai, Y., Xiang, Q.Y., Li, Q., Wang, J.O., Ibrahim, K., Cao, J.L., (2014).. Appl. Phys. Lett. 105.
Dee, C.F., Ahmad, Ishaq, Yan, Long, Zhou, Xingtai, Majlis, BurhanuddinYeop, 2011. Amorphization of ZnO nanowires by proton beam irradiation. NANO 6 (3), 259–263.
Ahmad, Ishaq, Yan, Long, 2009. Jinlong Gong, Dezhang Zhu "Graphite-to-amorphous structural transformation of multiwalled carbon nanotubes under proton beam Irradiation". Mater. Lett. 63, 1505–1507.
Ahmad, Ishaq, Yan, Long, Zhu, Dezhang, 2009. The electrical conductivity of carbon nanotube sheets by ion beam irradiation. Nucl. Instrum. Methods Phys. Res. B 267, 1779–1782.
Honey, S., Naseem, S., Ahmad, Ishaq, Maaza, M., Bhatti, M.T., Madhuku, M., 2017. Interconnections between Ag-NWs Build by Argon Ions Beam Irradiation. J. Nanomater. Mol. Nanotechnol. 6 (2), 1000213.
Honey, S., Ishaq, Ahmad, Madhuku, M., Naseem, S., Maaza, M., Kennedy, J.V., 2017. Nickel nanowires mesh fabricated by ion beam irradiation-induced nanoscale welding for transparent conducting electrodes. Mater. Res. Express 4, 075042.
Shehla, H., Naseem, S., Ishaq, A., Maaza, M., Bhatti, M.T., Wan, D., 2016. Large scale silver nanowires network fabricated by MeV hydrogen ($H^+$) ion beam irradiation. Chin. Phys. B 25, 046105.
Shehla, H., Ishaq, A., Yaqoob, K., Javed, I., Saira, R., Shahzad, N., Maaza, M., 2016. Ion beam irradiation-induced nano-welding of Ag nanowires. Micro Nano Lett. 11, 34–37.
Honey, Shehla, Khan, Shakil, Iqbal, Javed, Madhuku, M., Ahmad, Ishaq, Naseem, Shahzad, Malik, Maaza, 2015. Protons irradiation induced coalescence of silver nanowires. Curr. Nanosci. 11 (6), 792–796.
Ahmad, Ishaq, WaheedAkram, G. Husnain, Long, Yan, Xingtai, Zhou, 2011. Coalescence of multi-walled carbon nanotubes and their electronic conduction nano networks. Curr. Nanosci. 7 (5), 790–793.
Ahmad, Ishaq, Madhuku, M., Sadaf, Adeela, Khan, S., Hussain, Javaid, Awais Ali, D., Wang, S.Z., Ilyas, G., Mola, A., Waheed, M., Rasheed, A., 2017. Tailoring the structural and optical characteristics of InGaN/GaN multilayer thin films by 12 MeV Si ion irradiation. Mater. Sci. Semicond. Process.. 64, 95–100.
Xie, Wei, Li, Rui, Qingyu, Xu., 2018. Enhanced photocatalytic activity of Se-doped $TiO_2$ under visible light irradiation. Sci. Rep. 8, 8752.
Dette, Christian, Pérez-Osorio, Miguel A., Kley, Christopher S., Punke, Paul, Patrick, Christopher E., Jacobson, Peter, Giustino, Feliciano, Jung, Soon Jung, Kern, Klaus, 2014. $TiO_2$ anatase with a bandgap in the visible region. Nano Lett. 14, 6533–6538.
Khan, Mohammad Ehtisham, Khan, Mohammad Mansoob, Min, Bong-Ki, Cho, Moo Hwan, 2018. Microbial fuel cell assisted band gap narrowed $TiO_2$ for visible light-induced photocatalytic activities and power generation. Sci Rep. 8, 1723.